PRINT ISSN 1119-8362
Electronic ISSN 2659-1502

Full-text Available Online at
https://www.ajol.info/index.php/jasem
http://www.bioline.org.br/ja

J. Appl. Sci. Environ. Manage.
Vol. 27 (2) 283-289 February 2023

Adsorption of Methyl Orange and Amoxicillin from Water using Metal-organic Framework Prepared from Solvothermal Mixing of Zn ions and 1,4-Benzenedicarboxylic Acid Moieties

***UKACHUKU, S; AMAEBI, DE; DIKE, CI**

Department of Chemical Sciences, Faculty of Basic and Applied Science, University of Africa, Toru-Orua, Bayelsa State, Nigeria

**Corresponding Author Email: samuel.ukachuku@uat.edu.ng; Tel: +2348067984260*
Co-Authors Email: julietf912@gmail.com; Izibeyadike52@gmail.com

ABSTRACT: In this study, we determined the capacity of metal organic framework, which we prepared by the solvothermal mixing of Zn ions and 1,4-benzenedicarboxylic acid (Zn/BDC) moieties to adsorb methyl orange (MO), and amoxicillin (AMX). Results obtained show that MO and AMX adsorption capacity by Zn/BDC (mg/g) was found to increase with increase in solution concentration, for each contaminant type. Three isotherm models were applied to the adsorption data: Freundlich, Langmuir, and Temkin. R^2 values obtained for the adsorption of MO, 0.9778, 0.8589 and 0.9038 for Freundlich, Langmuir and Temkin plots respectively, indicates that all three models fit the adsorption data appreciably good, with the Freundlich isotherm providing the best fit. Those for AMX, 0.6737, 0.0616, and 0.5300 indicated a poor fit, but the Freundlich isotherm came out as best fitting isotherm for AMX, an indication of a multilayer adsorption process. Maximum possible amount of contaminant adsorbed per gram of Zn/BDC deduced from the Langmuir isotherm for the adsorption of both contaminants were 93.46 mg/g and 18.41 mg/g for MO and AMX respectively. This, among other indicators, showed the preference of Zn/BDC for MO relative to AMX. Adsorption kinetic models: pseudo first order, pseudo second order, and Weber-Morris intraparticle diffusion models, gave R^2 values that indicate that intraparticle diffusion dominated the adsorption of MO, while the adsorption of AMX followed pseudo second order kinetics, an indicator of chemisorptive mechanism. Calculated Q_e values, were in close agreement with experimental values.

DOI: **https://dx.doi.org/10.4314/jasem.v27i2.14**

Cite this paper as: UKACHUKU, S; AMAEBI, DE; DIKE, CI (2023). Adsorption of Methyl Orange and Amoxicillin from Water using Metal-organic Framework Prepared from Solvothermal Mixing of Zn ions and 1,4-Benzenedicarboxylic Acid Moieties. *J. Appl. Sci. Environ. Manage.* 27 (2) 283-289

Dates: Received: 26 January 2023; Revised: 11 February 2023; Accepted: 14 February 2023
Published: 28st February 2023

Keywords: azo dyes, antibiotics, batch adsorption, methyl orange, amoxicillin

In recent times, a global water pollution concern has arisen due to rapid increase in industrialization and urbanization. Pharmaceutical products and synthetic dyes are among emerging chemical stressors with immense potential to cause negative health and environmental impacts (Samal et al., 2022; Singh et al., 2021). These are all indispensable household consumables with daily global formulation volumes commensurate with population and demand. Dyes are colour imparting materials whose negative health and environmental impacts mainly arise from the presence of aromatic functions in their structures. Thus, they carry potential health and environmental threats of same magnitude as direct aromatic species. They also pose a threat to aquatic life by reducing the amount of penetrable sunlight radiation, being extremely colored (Lellis et al., 2019). Pharmaceuticals are wide range of products employed for health restoration purposes. Prescription drug class such as antibiotics are highly utilized by humans, and in veterinary medicine, which increases the possibility of their continuous contamination of water bodies and their concentrations growing to pollution levels (Polianciuc et al., 2020). Treatment of waste waters from hospitals

and pharmaceutical industries had attracted immense attention due to the number of negative environmental impacts of antibiotics as well as other drug formulations. Amongst the concerns are the possibility of causing antibiotic resistance in bacteria. Infection of humans by antibiotic resistant bacteria has direct consequences including delayed health recovery, morbidity and mortality (Merlin, 2020; Polianciuc et al., 2020). Further, antibiotics leaves persistent chemical residue in water, sediments and soil, which causes phytotoxicity, tissue toxicity and genotoxicity in worms, and bacteria (Chen et al., 2017; Timmerer et al., 2020; Dong et al., 2012). A number of effective methods to rid waste organic water of contaminants have been reported. They are: electro-degradation, photocatalytic degradation, advanced oxidation, adsorption, precipitation, coagulation-flocculation, ion-exchange, and biological treatment (Balarak et al., 2017; Chaba and Nomngongo, 2019). However, adsorption is the most utilized method since it is relatively cheap, offers efficiency in contaminants removal operation as well as design simplicity (Ferdowsi et al., 2015). Here a good number of adsorbents are being employed, including: activated carbons, zeolites, silica gel, and alumina. However, in recent times researchers are investigating a class of materials with nanosized pores as possible alternatives to the infamous adsorbents. These emerging materials include: dendrimers (Wazir et al., 2020), carbon nanotubes (Mashkoor et al., 2020), Zinc Oxide (Yuvaraja et al., 2018), covalent-organic frameworks (Rasheed, 2022), as well as metal-organic frameworks (Furukawa et al., 2014). Metal-organic frameworks (MOFs) are crystalline porous materials which originated from the pioneering works of Yaghi and Li in 1995 (Yaghi and Li, 1995). Their preparation mostly yields a self-assembled reticulated array of metal nodes, known as secondary building units, that are bridged by organic ligands. This array of building units and ligands leaves an open framework with specific topology, depending mainly on the coordination geometry of the metal. MOFs have large pore volume and ultrahigh surface area to mass ratio. These properties have been leveraged upon and applied in gas capture (Trickett et al., 2017), drug delivery (Maranescu and Visa, 2022) and aqueous adsorption of contaminants (Furukawa et al., 2014).In this study, we determined the capacity of metal organic framework, which we prepared by the solvothermal mixing of Zn ions and 1,4-benzenedicarboxylic acid moieties, to adsorb antibiotics and azo-dyes from water.

MATERIALS AND METHODS

Analytical grade reagents were employed for the study, including: $Zn(NO_3)_2 \cdot 6H_2O$ (Aladdin Biological Technology Co, LTD, Shanghai, China) benzene-1,4-dicarboxylic acid (Merck KGaA, Darmstadt, Germany), N,N-dimethylformamide (DMF) (Merck KGaA, Darmstadt, Germany), methanol (Merck KGaA, Darmstadt, Germany), and methyl orange dye (Kem light Laboratories PVT Ltd, Mumbai, India). Representative antibiotic, amoxicillin, was a capsule content prepared by ‘’me cure’’ industries Ltd, Lagos, Nigeria. The capsule was purchased from a local pharmaceutical store.

Preparation of amoxicillin stock solution: 200 mg/L Stock solution of amoxicillin was prepared by dissolving 0.2 g of the powder in 1 liter of sterile water. The mixture was sonicated for thorough dissolution using an intelligent ultrasonic processor (from Shangai Huxi Industry Co. Ltd, China).

Preparation of methyl orange stock solution: 200 mg/L Stock solutions of methyl orange was prepared by dissolving 0.20 g of the powder into 1 liter of sterile water. Again, the dissolution was enhanced with a sonicator.

*Variation of initial adsorbate concentration**:*** working solutions of concentrations: 10, 20, 30, 40 and 50mg/L were prepared from each of the stock solutions through serial dilution. All working concentrations for each of the two adsorbate solutions were validated with a single beam UV-Visible spectrophotometer (LI-285, a product of Lasany International, Panchkula, India). Batch adsorption tests were conducted in 100 ml beakers with 20 ml solution mixed with 0.01 gram of Zn/BDC MOF and agitated with a magnetic shaker at a speed of 100 rpm for 1-hour equilibration time. At the stop of each study, solution extract was analyzed with the single beam UV-Visible spectrophotometer using wavelengths of 229 nm and 465 nm for amoxicillin and methyl orange respectively.

Variation of adsorbate/adsorbent contact duration: To determine the performance of Zn/BDC MOF at various contact durations, adsorbent/adsorbate contact were maintained for the following times: 10, 20, 30, 40, and 50, minutes. For each batch, a Zn/BDC load of 0.01 g was mixed 30 mg/L solution. Each mixture was agitated with a magnetic shaker at a speed of 100 rpm. Extracts were analyzed using the single beam UV-Visible spectrophotometer.

RESULTS AND DISCUSSION

The results obtained from the variation of initial adsorbate concentration are presented in terms of adsorbed percentages and adsorbent capacity. Adsorbent capacity was estimated from the equation:

$$Q_e = \frac{(C_o - C_e)v}{w}$$

where Q_e, C_o, C_e, v, and w, are respectively adsorbent capacity, initial concentration of adsorbate, final concentration of adsorbate, volume of adsorbate solution used in the batch adsorption test, and weight of adsorbent used.

The plots in Figure 1 shows that percentages (secondary axis) of MO and AMX adsorbed onto Zn/BDC tends to decrease as solution concentration increases. Contrastingly, adsorption capacity of Zn/MOF (mg/g) (primary axis) increased steadily with increase in solution concentration. The observed higher sorption percentages for MO depict a slight adsorption preference of Zn/BDC for MO relative to AMX. This could be due to enhanced interaction of MO with the adsorbent, comparatively, as a result of a number of factors including: lower size, lower hydrophobicity, and higher motility (Table 1).

Table 1. Structure and properties of MO and AMX

Structure/Properties	**Methyl orange**	**Amoxicillin**
Structure	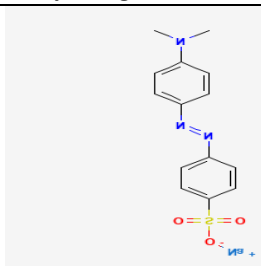	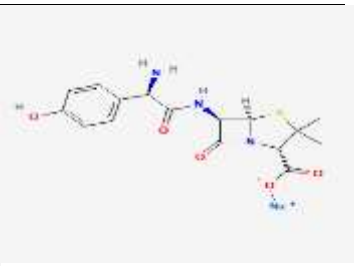
Molecular formula	$C_{14}H_{14}N_3NaO_3S$	$C_{16}H_{19}N_3O_5S$
Molecular Mass ($gmol^{-1}$)	327.33	365.4
Aqueous solubility (g/L) (20 ^{0}C, pH=5.6)	~ 5. 00 [a]	~ 3.43 [b]
Density (g/cm^3)	1.28	1.6
Molecular size (nm)	1.19 x 0.68 x 0.37 [c]	1.24 x 0.56 x 0.46 [b]

References: a ~ ("Methyl Orange," 2023), *b* ~ (Stuart et al., 2014), *c* ~ (Iwuozor et al., 2021)

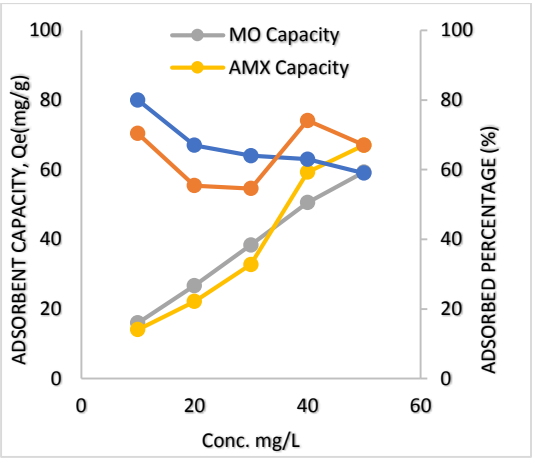

Fig 1: Plots of Adsorbent capacity/Adsorbed percentages against Initial adsorbate concentration

Linear forms of the Freundlich, Langmuir, and Temkin (Table 2) were applied to the experimental data to estimate the extent of adsorption of MO and AMX onto Zn/BDC. The isotherm plots are presented in Figures 2-4. All isotherm parameter values for the adsorption of both MO and AMX are presented in Table 3. R^2 values obtained for the adsorption of MO, 0.9778, 0.8589 and 0.9038 Freundlich, Langmuir and Temkin plots respectively, indicates that all three models fit the adsorption data appreciably good, however, for the adsorption of AMX, R^2 values of 0.6737, 0.0616, and 0.5300 for Freundlich, Langmuir and Temkin plots respectively, show a relatively poor fit. Freundlich comes out as the best fitting adsorption model in this system going by the R^2 values. This is indicative of the dominance of a multilayer adsorption process (Ukachuku and Abasi, 2021). However, in the Zn/BDC-MO sorption system, the positive values of the Langmuir isotherm constants, K_L (0.075 L/mg), Q_m (93.46 mg/g), and the separation factor, R_L (0.2), being $0 < R_L < 1$ (representing a favourable adsorption process), also depict a monolayer adsorption process. This is not the case with the Zn/BDC-AMX sorption system, as shown by its poor Langmuir R^2 value. Further, Q_m represent the maximum possible amount of MO or AMX that can be taken by one gram of Zn/BDC. The higher Q_m values, 93.46 mg/g, obtained from the Zn/BDC-MO sorption system relative to that obtained from the Zn/BDC-AMX sorption system, 18.41 mg/g, only show that Zn/BDC adsorbed MO better than AMX. This is also revealed by the higher Freundlich constant, K_F (which also represents adsorption capacity (Ukachuku and Abasi, 2021)). From Table 3, we see that K_F(MO) > K_F(AMX). The Temkin isotherm can be applied to estimate the heat of adsorption of an adsorption system (Ayawei et al., 2017). The Temkin isotherm parameter, b_T, is related to the heat of adsorption by the relation:

$$b_T = \Delta Q = -\Delta H,$$

where b_T, ΔQ, and ΔH are the adsorption potential, heat of adsorption and enthalpy change respectively (Ukachuku and Abasi, 2021). Using the aforementioned relation, the heats of adsorption, ΔH, from the b_T values are: -134.82 Jmol^{-1} and -98.14 Jmol^{-1}, for MO and AMX respectively, which implies that adsorption of MO and AMX onto Zn/BDC are both exothermic processes.

Table 2: Linearized Isotherm Models

Model	***Linear equation***
Freundlich	Ln Q_e = Ln K_F + $\frac{1}{n}$ Ln C_e
Langmuir	$\frac{C_e}{Q_e} = \frac{C_e}{Q_m} + \frac{1}{K_L Q_m}$
Temkin	Q_e = B *Ln* A + B *Ln* C_e

Table 3: Values of Adsorption Isotherm Parameters for the Adsorption of Mo and Amx onto Zn/Bdc Mof

Freundlich Isotherm			**Langmuir Isotherm**			**Temkin Isotherm**		
Parameters	**MO**	**AMX**	**parameters**	**MO**	**AMX**	**parameters**	**MO**	**AMX**
N	1.74	1.23	Q_m(mg/g)	93.46	18.41	b_T(Jmol^{-1})	134.82	98.14
K_F (mg/g)	10.13	5.5	K_L (L/mg)	0.075	0.233	A(Lg^{-1})	0.94	1.93
R^2	0.9778	0.6737	R^2	0.8589	0.0616	R^2	0.9038	0.5300
			R_L	0.20	0.08			

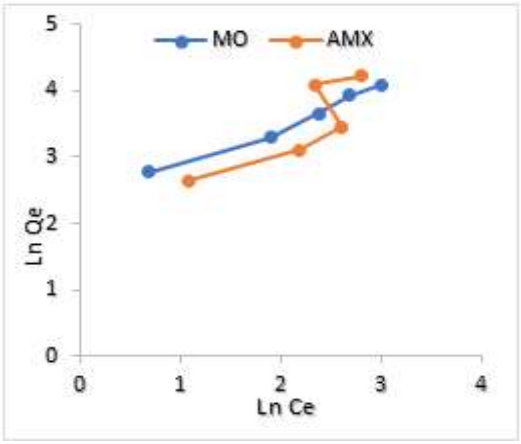

Fig 2: Freundlich Isotherm Plots

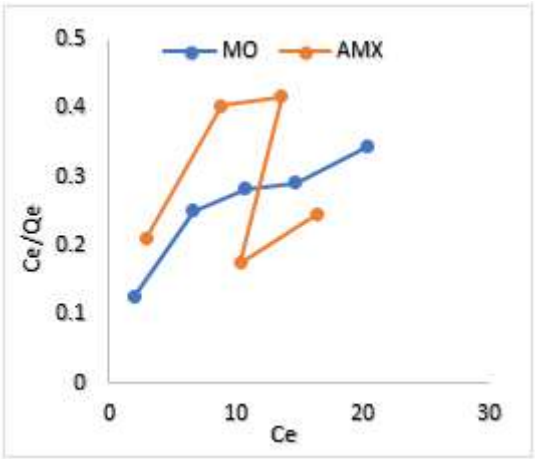

Fig 3: Langmuir Isotherm Plots

Three adsorption kinetic models were applied for the data obtained from contact time studies including: pseudo first order, pseudo second order, and Webber-Morris intraparticle diffusion models. The linear equations are presented in Table 4. The adsorbent capacity at various contact times, Q_t, was obtained by:

$$Q_t = \frac{(C_o - C_t)v}{w}$$

Where Q_t, C_o, C_t, v, w, are the adsorbent capacity at the studied time interval, initial concentration of adsorbate, adsorbate concentration at time, t, volume of solution, and weight of adsorbent respectively.

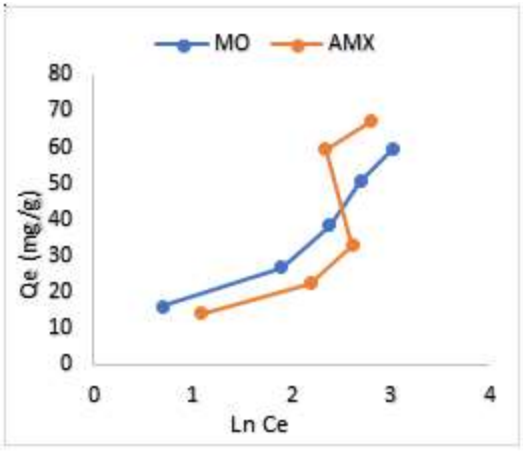

Fig 4: Temkin Isotherm Plots

Kinetic models are useful in the prediction of likely mechanism of interaction between adsorbent and adsorbate. The parameters deduced from the employed kinetic models are presented in Table 5.

Table 4: Adsorption Kinetic Models

Kinetic model	**Linear equation**
Pseudo first order	$Ln(q_e - q_t) = Ln\ q_e - k_1 t$
Pseudo second order	$\frac{t}{q_t} = \frac{1}{k_2 q_e^2} + \frac{t}{q_e}$
Webber-Morris Intraparticle diffusion	$q_t = k_{i.d}\ t^{1/2} + X$

The kinetic plots are presented in Figures 5 to 7. The R^2 values obtained for adsorption of MO were 0.9156, 0.9943, and 0.9947 for pseudo first order, pseudo

second order, and Weber-Morris intraparticle diffusion models respectively, thus depicting, by highest R^2 value, the dominance of intraparticle diffusion in its adsorption. For AMX, the R^2 values 0.7704, 0.9583, and 0.8771 for pseudo first order, pseudo second order, and Weber-Morris intraparticle diffusion models respectively, reveal the dominance of pseudo second order kinetics in its adsorption, as shown by the R^2 value, thus, suggesting a chemisorptive exchange of ions in the adsorption process (Guo et al., 2014). The Q_e values calculated from the pseudo first order are 44.74 mg/g (MO), 42.44 mg/g(AMX), those from the pseudo second order are 55.25 mg/g (MO), 54.64 mg/g (AMX). Both sets of Q_e values are somewhat in agreement with the experimental values, 39.92mg/g (MO) and 42.87 mg/g (AMX), however, the pseudo first order values are closer.

Table 5: Parameters from Adsorption Kinetic Models for Adsorption of Mo and Amx onto Zn/BDC

Pseudo First Order			**Pseudo Second Order**			**Intraparticle Diffusion**		
Parameters	**MO**	**AMX**	parameters	**MO**	**AMX**	parameters	**MO**	**AMX**
q_e (mg/g)	44.74	42.44	**q_e (mg/g)**	55.25	54.64	***X* (mg/g)**	8.79	6.41
k_1 (min^{-1})	0.0681	0.0704	**k_2 (g mg^{-1} min^{-1})**	0.0009	0.0012	**$k_{i.d}$ (mg $g^{-1}min^{-1/2}$)**	4.32	5.27
R^2	0.9156	0.7704	**R^2**	0.9943	0.9583	**R^2**	0.9947	0.8771

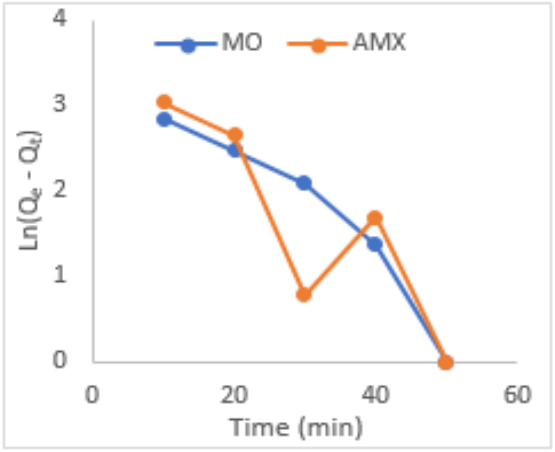

Fig. 5: Pseudo First Order plots

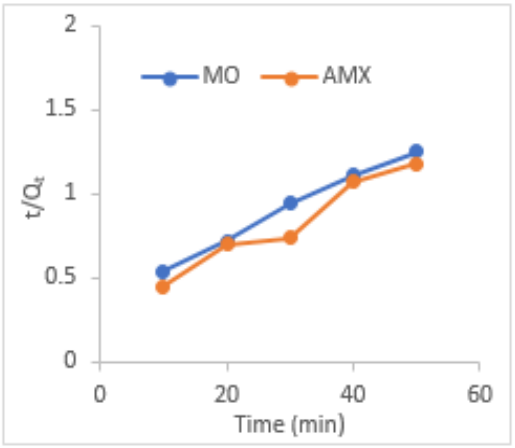

Fig. 6: Pseudo Second Order plots

Pseudo firs order kinetics describes a physiosorptive processes involving non-bonding forces (Chitongo et al., 2019). This may have also contributed to the adsorption process for both MO and AMX, as shown by both the Q_e values and the fairly high R^2 values. The Weber-Morris intraparticle diffusion model is adjudged as the rate limiting step if the plot passes through the origin (Kang et al., 2021). Further, the number of jointed lines in the plots gives the number of steps of diffusion of particles through the adsorbent's pores (Ukachuku and Abasi, 2021). The intraparticle diffusion plots for MO, Fig 7, is a single line, thus, showing that intraparticle diffusion is the rate limiting step in the adsorption of MO onto Zn/BDC. For AMX, a bilinear plot can be noticed, which indicate a two-step mechanism, and evidence that intraparticle diffusion was not the rate limiting step (Ukachuku and Abasi, 2021).

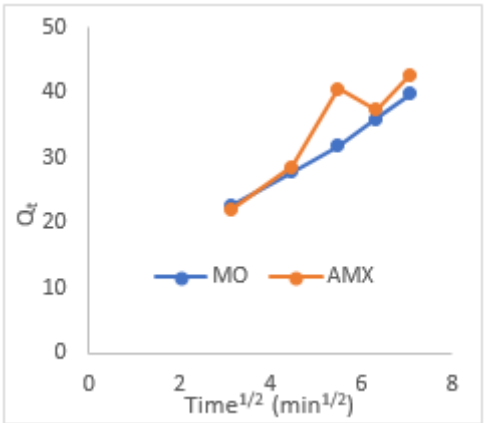

Fig. 7: Weber-Morris Intraparticle diffusion plots

Conclusion: The study has demonstrated, that Zn/BDC (prepared through the solvothermal blending of Zinc and benzene-1,4-dicarboxylic acid) can be effective as adsorbent of methyl orange and amoxicillin in aqueous media. This will benefit waste water management in pharmaceutical, textile and related industries. Conclusively, the outcome of the

study is an indication of a clear pathway to tackling those concerns arising from the presence of azo dyes and antibiotics in the environment.

Acknowledgment: The authors would like to appreciate the management of the University of Africa, Toruorua, as well the Laboratory Technologists in the Department of chemical sciences for granting permission and access to the Laboratory, as well as providing technical support.

REFERENCE

Ayawei, N; Ebelegi, AN; Wankasi, D (2017). Modelling and Interpretation of Adsorption Isotherms. *J. Che.* 2017:1–11.

- Balarak, D; Joghatayi, A; Mostafapour, F; Azarpira, H (2017). Biosorption of amoxicillin from contaminated wateronto palm bark biomass. *Int. J. L. Sci.Pharm. Res.* 7(1): 9-16

Chaba, JM; Nomngongo, PN (2019). Effective adsorptive removal of amoxicillin from aqueous solutions and wastewater samples using zinc oxide coated carbon nanofiber composite. *Emerg. Cont.* 5: 143–149.

Chen, C. Q; Zheng, L; Zhou, JL; Zhao, H (2017). Persistence and risk of antibiotic residues and antibiotic resistance genes in major mariculture sites in Southeast China. *The Sci. Tot. Environ.* 580: 1175–1184.

Chitongo, R; Opeolu, BO; Olatunji, OS (2019). Abatement of Amoxicillin, Ampicillin, and Chloramphenicol From Aqueous Solutions Using Activated Carbon Prepared From Grape Slurry. *CLEAN – S. A., Wat.*, 47(2): 1800077.

Dong, L; Gao, J; Xie, X; Zhou, Q (2012). DNA damage and biochemical toxicity of antibiotics in soil on the earthworm Eisenia fetida. *Chemos.* 89(1): 44–51.

Ferdowsi, R; Layali, I; Mostafa, K (2015). Treatment Of Antibiotics From Wastewater By Adsorption Onto Low Adsorbent. *Int. J. Anal. Pharm. Biomed. Sci.* 4(9): 44-50

Furukawa, H; Gándara, F; Zhang, Y-B; Jiang, J; Queen, WL; Hudson, MR; Yaghi, OM (2014). Water Adsorption in Porous Metal–Organic Frameworks and Related Materials. *J. Ame. Chem. Soc.* 136(11): 4369–4381.

Guo, X; Du, B; Wei, Q; Yang, J; Hu, L; Yan, L; Xu, W (2014). Synthesis of amino functionalized magnetic graphenes composite material and its application to remove Cr(VI), Pb(II), Hg(II), Cd(II) and Ni(II) from contaminated water. *J. Hazard. Mater*. 278: 211–220.

Iwuozor, KO; Ighalo, JO; Emenike, EC; Igwegbe, CA; Adeniyi, AG (2021). Do Adsorbent Pore Size and Specific Surface Area Affect The Kinetics of Methyl Orange Aqueous Phase Adsorption*?* [Preprint]. In Review. https://doi.org/10.21203/rs.3.rs-777328/v1

Kang, X; Liu, Y; Yang, C; Cheng, H (2021). Removal of amoxicillin from aqueous solution using sludge-based activated carbon modified by walnut shell and nano-titanium dioxide. *J. Wat. Reu. Desal.* 11(1): 97–109.

Lellis, B; Fávaro-Polonio, CZ; Pamphile, JA; Polonio, JC (2019). Effects of textile dyes on health and the environment and bioremediation potential of living organisms. *Biotech. Res. Innovat.* 3(2): 275–290.

Maranescu, B; Visa, A (2022). Applications of Metal-Organic Frameworks as Drug Delivery Systems. *Int. J. Mol. Sci*. 23(8): 4458.

Mashkoor, F; Nasar, A; Inamuddin (2020). Carbon nanotube-based adsorbents for the removal of dyes from waters: A review. *Environ. Che. Let.* 18(3): 605–629.

Merlin, C (2020). Reducing the Consumption of Antibiotics: Would That Be Enough to Slow Down the Dissemination of Resistances in the Downstream Environment? *Front. Microbiol*. *11*.

Methyl orange (2023). In *Wikipedia*. https://en.wikipedia.org/w/index.php?title=Methyl_orange&oldid=1131417160

Polianciuc, SI; Gurzău, AE; Kiss, B; Ștefan, MG; Loghin, F (2020). Antibiotics in the environment: Causes and consequences. *Medicine and Pharmacy Reports*. https://doi.org/10.15386/mpr-1742

Rasheed, T (2022). Covalent organic frameworks as promising adsorbent paradigm for environmental pollutants from aqueous matrices: Perspective and challenges. *Sci. Tot. Env*. 833: 155279.

Samal, K; Mahapatra, S; Hibzur AM (2022). Pharmaceutical wastewater as Emerging Contaminants (EC): Treatment technologies, impact on environment and human health. *Energ. Nex.* 6: 100076.

Singh, J; Gupta, P; Das, A (2021). Dyes from Textile Industry Wastewater as Emerging Contaminants in Agricultural Fields. In V. Kumar Singh, R. Singh, & E. Lichtfouse (Eds.), *Sust. Agric. Rev.* 50*: Emerg. Cont. Agric*. Spring. Int. Pub. 2021: 109–129.

Stuart, AV; Zuo, J; Löbenberg, R (2014). Investigating the dissolution profiles of amoxicillin, metronidazole, and zidovudine formulations used in Trinidad and Tobago, West Indies. *AAPS PharmSciTech*, 15(5): 1060–1069.

Timmerer, U; Lehmann, L; Schnug, E.; Bloem, E (2020). Toxic Effects of Single Antibiotics and Antibiotics in Combination on Germination and Growth of Sinapis alba L. *Plant.* 9(1): 107.

Trickett, C. A., Helal, A., Al-Maythalony, B. A., Yamani, Z. H., Cordova, K. E; Yaghi, O. M. (2017). The chemistry of metal–organic frameworks for CO2 capture, regeneration and conversion. *Nat. Rev. Mater.* 2(8): 17045.

Ukachuku, S; Abasi, CY (2021). Solid-Liquid sorption studies of Ni, Cd, and Pb on unmodified and modified avocado pear seed. *Ann. Appl. Sci*. 7(2): 23–28.

Wazir, MB; Daud, M; Ali, F; Al-Harthi, MA (2020). Dendrimer assisted dye-removal: A critical review of adsorption and catalytic degradation for wastewater treatment. *J. Mole. Liq.* 315:113775.

Yaghi, OM; Li, H (1995). Hydrothermal Synthesis of a Metal-Organic Framework Containing Large Rectangular Channels. *J. Ame. Chem. Soc.* 117(41): 10401–10402.

Yuvaraja, G; Prasad, C; Vijaya, Y; Subbaiah, MV (2018). Application of ZnO nanorods as an adsorbent material for the removal of As(III) from aqueous solution: Kinetics, isotherms and thermodynamic studies. *Int. J. Ind. Che.* 9(1): 17–25.